

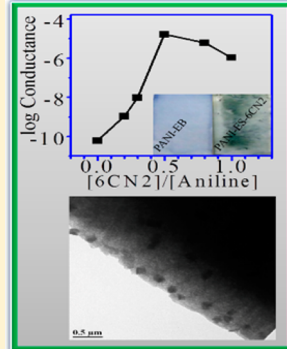
Doping of Polyaniline with 6-Cyano-2-naphthol

Debasree Das, Anindya Datta,* and Aliasgar Q. Contractor*

Department of Chemistry, Indian Institute of Technology Bombay, Powai, Mumbai 400076, India

S Supporting Information

ABSTRACT: The conductivity of polyaniline (PANI) is ascribed to its emeraldine salt (PANI-ES), which is formed by protonation of its emeraldine base (PANI-EB) by acids. Generally, mineral acids are used for this purpose, but the use of dopants and additives to maintain the required acidity provides an alternative method to the preparation of PANI-ES. The present work attempts to achieve the protonation by the use of a weak organic acid, namely, 6-cyano-2-naphthol (6CN2), which is generally used as a superphotoacid, as its excited state pK_a is significantly smaller than its ground state pK_a . The question here is if the protonation of the aniline moieties in PANI takes place and if it does, whether it takes place by dissociation of the ground state or the excited state of 6CN2. Room temperature conductance measurements were carried out to see the effect of doping. The formation of PANI-ES from PANI-EB has been monitored by UV-vis spectrophotometry. When a polar counterion is inserted into the polymer matrix, it changes the environment of the nearby chains by introducing defects, reorganization of charges as a result of interaction with the polymer. Morphological investigation was done using optical microscopy, field emission gun scanning electron microscopy (FEGSEM), and field emission gun transmission electron microscopy FEGTEM. The influence of 6CN2 on the crystallinity of the polymer was determined by X-ray diffraction (XRD).



INTRODUCTION

Polyaniline (PANI) behaves like a semiconductor by virtue of its highly conjugated π delocalized backbone. It has a plethora of applications in the field of electrochromic devices, drug delivery, sensor applications, and rechargeable batteries.^{1–3} These applications generally depend upon the switching between the different states of polymer, namely, leucoemeraldine, emeraldine, and pernigraniline states,^{2,3} as a response to chemical or electrical inputs. PANI can be synthesized chemically or electrochemically with or without the support of template. PANI-based nanostructures exhibit enhanced chemical sensitivity, water dispersibility along with the introduction of new properties like molecular memory and photothermal effect.² PANI exhibits environmental stability, reversible switching between states, ease of synthesis, processability, high conductivity, and other optical properties.³

Acid/base doping of PANI is a commonly used modality and has received great attention.^{4–6} The present paper involves two forms of PANI, namely, the emeraldine base (PANI-EB) and the emeraldine salt (PANI-ES) with literature reported conductivities of 10^{-10} and $>1\text{ S cm}^{-1}$, respectively.² It is known that these two forms can be interconverted by doping/dedoping, and this is reflected in switching of electrical conductivity of the polymer.⁷ It can be done either by casting films or by immersing the PANI-EB in acid solutions.⁸

Upon doping with mineral acids, imine nitrogen groups in PANI-EB get protonated to yield the conducting PANI-ES form. Secondary dopants like *p*-cresol, 2-chlorophenol, 3-ethylphenol, 2-fluorophenol, etc. further augment the conductivity of acid-doped PANI, despite being inert themselves.⁴ Lewis acids like SnCl_4 ,⁹ salts of Li^+ ,^{10,11} transition metal salts

like EuCl_3 ,¹² etc. have also been used as dopants instead of mineral acids. Inorganic oxides like SnO_2 ,¹³ Al_2O_3 , ZnO , TiO_2 ,¹⁴ Mn_3O_4 ,¹⁵ form composites with PANI, in which the two distinct phases exist, one for each of the materials. Other than inorganic acids, organic acids like *m*-cresol, D,L-camphorsulfonic acid (CSA), dodecylbenzenesulfonic acid (DBSA) and other substituted phenols, carboxylic,^{16,17} sulfonic,^{18,19} acetic, and oxalic acids have been used as organic acid dopants in different studies.²⁰ Dissociation of these acids within the polymer provides the acidic microenvironment necessary for protonation of the imine nitrogen and consequent formation of the emeraldine salt, usually accompanied by structural rearrangement and distribution of charges throughout the polymer chain. Carbon nanotubes²¹ and graphene²² have been used as dopants, to increase the conductivity of PANI. In the present submission, we have explored the conductivity, crystallinity, morphology, and fluorescence properties of PANI films doped noncovalently with 6-cyano-2-naphthol (6CN2). The reason behind choice of 6CN2 is 2-fold. It is a weak acid as well as fluorophore and is known to be a superphotoacid, with an excited state pK_a of 0.2 and a ground state pK_a of 8.4.^{23–25} Most of the earlier work with naphthol compounds has been performed with chemically synthesized copolymers^{26,27} of 1-amino-2-naphthol-4-sulfonic acid with aniline. Electrochemically synthesized layers of PANI and poly-1-naphthol have been investigated for potential applications in rechargeable batteries.²⁸ The motivation for the study is

Received: June 18, 2014

Revised: October 19, 2014

Published: October 21, 2014



to find out if 6CN2 is a good enough acidic dopant to bring about the formation of PANI-ES and if so, whether the protonation is caused by the ground state or the excited state of the dopant. The importance of protonation by ground state has been discussed already.^{16–20} Protonation from the excited state, if observed, would have profound implications in photoconductivity of PANI, which is interesting from the point of view of designing devices.²⁹

■ EXPERIMENTAL SECTION

Materials. PANI-EB (average MW of ~5000) and 6CN2 were purchased from Sigma Aldrich. N-Methyl-2-pyrrolidone (NMP), Triton X-100, and absolute ethanol (99.9%) were purchased from Sisco Research Laboratories Pvt. Ltd., India, and Fisher Scientific, Brampton, Ontario Canada respectively. Emparta grade NaOH was purchased from Merck Specialties Private Limited.

Preparation of Electrodes. Two gold contacts as shown in Figure 1 with a separation of 40 μm were made by lithography.

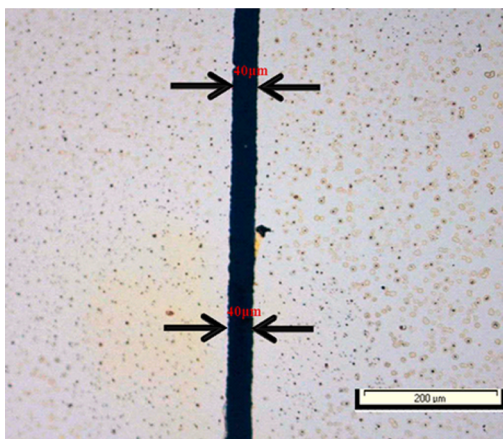


Figure 1. Optical microscopy of glass slide showing an etched line of 40 μm (approximately) width separating the two gold contact pads at 10 \times magnification.

The 30 nm of chromium layer and 100 nm of gold layer were deposited by physical vapor deposition on 1 cm \times 1 cm glass slides using HINDHIVAC (model 12A4D) thermal evaporator. Glass slides were pretreated with Triton X-100 before deposition.

Doping of PANI-EB. PANI-EB was dissolved in NMP and stirred overnight under nitrogen atmosphere. Then it was filtered through a 0.45 μm filter. 6CN2 was added to this filtered solution. PANI-EB was doped by adding appropriate amounts of 6CN2 in the range of a molar ratio of 0 to 1:1 of 6CN2/aniline. Then 10 μL of solutions with and without 6CN2 were drop cast on the gold coated patterned glass slides. Then these samples were vacuum-dried in an oven at 50 °C for 8 h.

Characterization. Electrical Characterization. The 10 μL solutions of various compositions with and without 6CN2 were drop-cast on the gold coated patterned glass slides. These samples were further vacuum-dried in an oven at 50 °C for 8 h. Conductance was measured using a Keithley 4200-SCS semiconductor characterization system. Sample preparations were carried out in the dark for conductance measurements under illumination with a mercury lamp.

Imaging of Samples. The morphology of the as-prepared samples was investigated using an Olympus microscope (MX61). Electron microscopy of the same samples was done in JEOL JSM 7600F. For FEGSEM a thin coating of platinum was given to avoid charging using JEOL JFC-1600 auto fine coater. Thickness measurements were done with cross-sectional FEGSEM.

FEGTEM was carried out in JEOL JEM 2100F. For FEGTEM, the samples were prepared by scraping the film deposited on a glass slide and dispersing in ethanol by ultrasonication. A drop of the sonicated ethanol suspension was placed on a carbon-coated copper grid and vacuum-dried overnight.

Structural Investigation of Samples. For XRD, samples were deposited on glass slides in the same manner as mentioned above and vacuum-dried before measurements. All the samples were measured in SmartLab X-ray diffractometer Rigaku within the scanning range of $2\theta = 5\text{--}40^\circ$ for all the measurements.

Absorbance and Fluorescence Spectroscopy Measurements. For spectroscopic measurements 20 μL of PANI-EB, 6CN2, 6CN2 doped emeraldine salt form of PANI (PANI-ES-6CN2) was spin coated individually on separate quartz slides at 2000 rpm for 20 s with the help of a spin coater (model WS-650 MZ-23 NPP/LITE) from Laurell Technologies Corporation. Quartz slides were cleaned with 10% solution of Triton X-100, Milli-Q water, and ethanol before use. The spin coated samples were vacuum-dried at 50 °C before measurements. Absorption and fluorescence were measured with PerkinElmer Lambda 25 and PerkinElmer LS 55, respectively. Spin coated samples were used, as drop-cast films were found to be too thick for transmission. A solid state accessory was used for the fluorescence measurements. For pH dependent study chloride solutions and phosphate buffers were used.

■ RESULTS AND DISCUSSION

Formation and Characterization of PANI-ES-6CN2. The $I\text{--}V$ plots of the films were linear, indicating ohmic behavior (Figure 2a). The electrical conductance of the composites is calculated from the slope of $I\text{--}V$ plots. The conductance of PANI-EB was very small (6.157×10^{-11} S).

It increased remarkably with progressive addition of 6CN2 and was significantly higher than the film doped with 2-naphthol (Figure 2a and Figure 2b). The maximum value of conductance (slope of the $I\text{--}V$ plot) was 1.654×10^{-5} S, at a 6CN2/aniline ratio of 0.5:1. For higher degrees of doping, conductance decreased to 1.074×10^{-6} S. The significant increase in conductance of PANI, by 6 orders of magnitude, demonstrates the effectiveness of 6CN2 as a conductance-enhancing dopant. The enhancement in conductance is not as much as that induced by inorganic acids but is comparable to that induced by other organic dopants. The organic dopants are larger in size and hence generate more defects and disorder in the polymer matrix¹⁷ and thus give lower electrical conductance. The most likely mechanism of enhancement of conductance by 6CN2 involves the dissociation of the O–H bonds of the naphtholic OH groups of 6CN2 molecules, which is a mildly acidic compound ($\text{pK}_a = 8.4$). The protons thus generated can get attached to the quinoid nitrogen atoms of PANI-EB, leading to the formation of PANI-ES-6CN2.

For comparison, the experiments were repeated with 2-naphthol. Even in this case, the conductance increased significantly, but to a lesser extent than in 6CN2, and seemed to be consistent with the fact that the pK_a of 2-naphthol is 9.45.

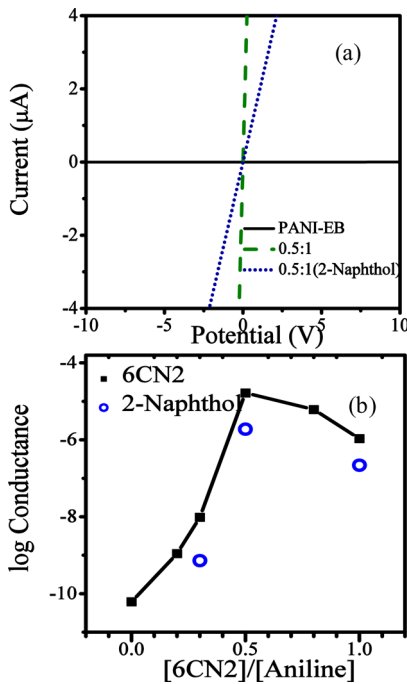


Figure 2. (a) I – V characterization plot. (b) Plot of conductance in S at different mole ratios measured at room temperature.

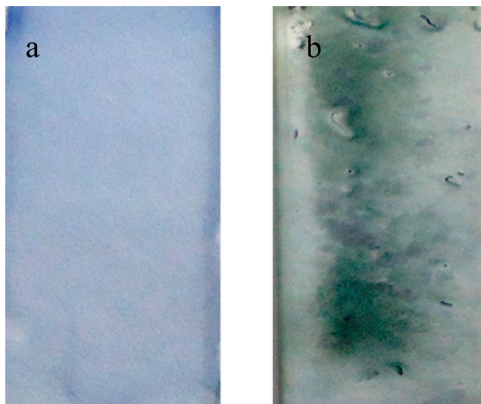


Figure 3. Photographs of PANI that was spin-coated on quartz slides in the (a) absence and (b) presence of 6CN2 as a dopant.

This control experiment lends credence to the possibility of an acid–base reaction being responsible for the observed increase in conductance of PANI doped by 6CN2, as 6CN2 is a stronger acid than 2-naphthol. As a superphotoacid, 6CN2 exhibits excellent excited state proton transfer (ESPT) properties.^{24,25} The ground state pK_a values of 6CN2 and 2-naphthol are 8.40 and 9.45, respectively. The excited state pK_a^* values of 6CN2 and 2-naphthol are 0.2 and 2.8, respectively. For 2-naphthols proton transfer in the excited state requires water molecules.²⁴ Thus, proton transfer is not possible in organic solvents. When the cyano group is attached to 2-naphthol, the ground state pK_a value decreased because of the introduction of the electron withdrawing group. Similarly the excited state pK_a^* values also decreased.²⁴ Apart from that substituted naphthols are found to show ESPT in nonaqueous solvents. Tolbert et al. have described that the ESPT in 2-naphthol takes place only through Grotthuss chain mechanism, whereas the same mechanism is not followed for ESPT by 6CN2. When the pK_a values were determined, the excited state pK_a^* values decreased to a greater

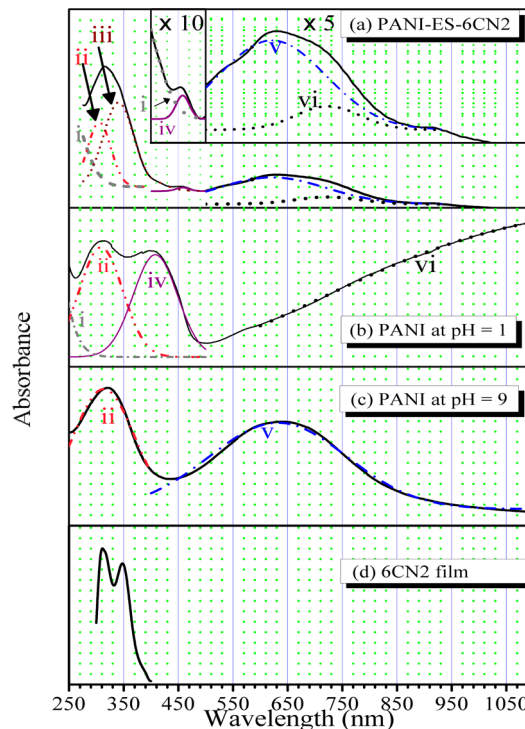


Figure 4. Absorption spectra of (a) PANI-ES-6CN2, (b) PANI at pH 1, (c) PANI at pH 9, (d) 6CN2 film. The spectra in (a) to (c) have been fitted to sums of Gaussian functions, and the component bands are assigned as (i) high energy transition, whose origin is not determined, (ii) π – π^* (PANI) band (in (a), some contribution from neutral (6CN2) could also be present), (iii) 6CN2 anion, (iv) polaron band to π^* band transition, (v) charge transfer between benzenoid and quinonoid moieties, (vi) π band to polaron band transition curve.

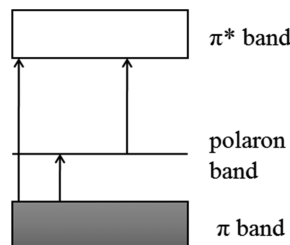


Figure 5. Band structures of PANI–ES form (adapted from ref 35).

extent than the ground state values.²⁴ However, it may be noted that one of the take home messages of the present work is that the pK_a values are not directly relevant here, as the medium is a solid, nonaqueous one. This has been discussed in detail under the proposed mechanism.

Evidence of the protonation of the nitrogen atoms of the aniline moieties is obtained in the form of color and then in the absorption spectra of the 6CN2 doped PANI. The color of the undoped (Figure 3a) as well as 6CN2 doped PANI solution in NMP as well as the PANI film is blue, indicating that the polymer is predominantly in the PANI-EB form. Upon vacuum drying at 50 °C, however, the color of 6CN2 doped PANI changes to bluish green (Figure 3b). This indicates the formation of the PANI-ES form generated after heating to some extent.³⁰ Notably, the film remained blue in the absence of doping by 6CN2 (Figure 3a). The bluish green color of the film may be attributed to the formation of PANI-ES, formed by taking up protons from 6CN2, which acts as an organic acid.

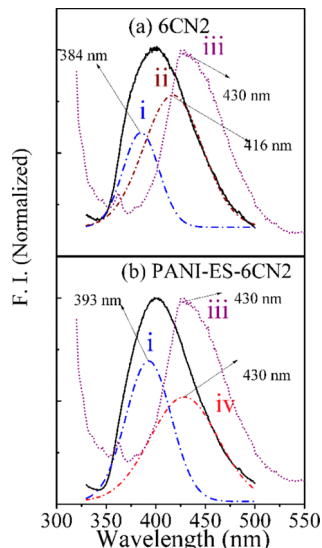


Figure 6. Fluorescence of (a) 6CN2 and (b) PANI-ES-6CN2. The spectra have been given Gaussian fits, and the bands are assigned as (i) neutral (6CN2) band, (ii) component of neutral (6CN2) band, (iii) 6CN2 anion band (naphthalate anion in dry state prepared from 1 M NaOH), and (iv) 6CN2 anion band.

Similar observations have been reported earlier with inorganic⁴ and organic acids.^{16–20}

The absorption spectra have been fitted to linear sums of two or more Gaussian functions (Figure 4a–c) in order to identify the relative contributions of 6CN2 and PANI to the spectra. The change in color of the polymer upon doping is manifested in a quantitative manner in the electronic absorption spectra. PANI-EB has two peaks: one at 320 nm due to $\pi-\pi^*$ transition and another at 630 nm ascribed to transitions arising from inter- or intramolecular charge transfer processes taking place between benzenoid and quinoid ring, leading to a formation of exciton.²⁹

Several theoretical studies have been carried out to understand the formation of the exciton in PANI. Conjugation in the PANI-EB form is hindered because of the quinoid structure in between the chains. It is known from the literature that the band at 2.0 eV originates from an exciton transition. The low energy of this transition compared to the other transition of the emeraldine base form indicated that the electron–hole moiety is not localized over a single phenyl ring.³¹ CNDO/S3 calculations are carried out by Duke et al. to understand the formation of exciton.³¹ It was found that the ground state configuration and the excited state configuration of the polymer are quite different. The electron is located at the quinoid moiety, while the holes are located at the two benzenoid rings. The quinoid moiety gets rotated by an angle of 90° with respect to its ground state form. The absorption band originates from formation of a local conformation with a distortion with respect to the ground state conformation. The electron hole pair is confined to a distorted part of the oligomer. This was further supported by disappearance of this band and appearance of new bands at 1.5 and 2.9 eV from the formation of polaron.³¹ Our observed values are 310 nm (4.0 eV), 450 nm (2.75 eV), 630 nm (1.97 eV), and 730 nm (1.69 eV) for PANI-ES-6CN2. Recent studies concentrate on the open structure of the polymer. Zhang et al. explored the effect of electric field on the exciton considering the open chain structure of the polymer. They considered the exciton to be

discrete and not self-trapped. In their model the authors considered a negative polaron at the end of the chain and a positive polaron at the middle of the chain.³² This corresponds to the transition at 630 nm with a band gap of approximately 1.97 eV in PANI-EB. This exciton transition was found to depend on torsional angle of phenyl rings, chain defects, and chain length as described by Dimitriev et al.³³

On doping of PANI with acids, there is a change in energy levels of the electronic band. Along with the decrease in absorbance there is also a red shift in the 630 nm band of PANI-EB when it is doped with 6CN2 as observed in Figure S2a,b (see Supporting Information).³⁴ It is due this change in energy that a red shift is observed in the spectra, Figure S2b signifying the conversion of PANI-EB to PANI-ES upon doping with 6CN2. There is also an appearance of a new band centered on 450 nm as new mid gap states are formed in the polymer. These bands are formed as transitions take place from the valence bands to the polaron band as shown in Figure 5.^{29,35} The absorption in the 700–1000 nm region (obtained from PANI-ES-6CN2 from that of PANI-EB denoted as PANI-ES-6CN2–PANI-EB) corresponds to the π band to the polaron band transition as shown in the inset of Figure S2a.

The Gaussian multipeak fitting from 250 to 400 nm region ($R^2 = 0.999$ where R^2 represents goodness of fit) shows the presence of three peaks (Figure 4a). The peak below 260 nm has not been taken into consideration, as our components are not expected in this region (Figure 4a). The peak around 310 nm region could be interpreted as originating from $\pi-\pi^*$ band of PANI-ES as well as neutral absorption band of 6CN2. Since these two bands are very close in energy, it is not possible to resolve the band into two separate peaks. The band at 340 nm originates from the anion absorption from 6CN2. For further confirmation a spectrum was recorded in a solid film obtained by evaporating NMP from the 6CN2 solution (Figure 4d). This spectrum shows the presence of the band near 300 and 340 nm corresponding to the neutral and anion absorption, respectively. From Figure 4a the band near 450 nm ($R^2 = 0.999$) was identified as discussed before. Two bands are also observed between 500 and 900 nm region ($R^2 = 0.997$). The origin of the band at 630 nm has already been discussed. The resolved spectra Figure 4a contain a band at 730 nm. Xia et al. mentioned the band at 780 nm arises when PANI-EB was doped with camphorsulfonic acid (HCSA).³⁵ As the difference spectrum shows a signature band from 700 to 1000 nm and from component analysis a band at 730 nm is observed, it could be explained that some amount of coil-like conformation may exist from the transition between π band to polaron band.³⁵ The 730 nm band could be due to the formation of coiled chains of PANI on preparing it from NMP. It is also reported when films have been prepared by casting from various solvents; several types of interactions originate affecting the structure and the properties of PANI.³⁶ The coil-like conformation arises when there are twists defects present in the aromatic rings. How the absorption changes with pH has been shown in Figure S3 (see Supporting Information). To further demonstrate the formation of PANI-ES-6CN2, the component analysis of PANI-ES at pH 1 was carried out. When Figure 4b ($R^2 = 0.995$) was compared with Figure 4a, no band at 340 nm was observed. In Figure 4a the contribution from the band at 340 nm was found to be higher than 310 nm band. These results indicate the conversion of PANI-EB to PANI-ES-6CN2. Figure 4b shows a band at 410 nm due to transition originating from the mid gap states. For Cl⁻ doped PANI a free

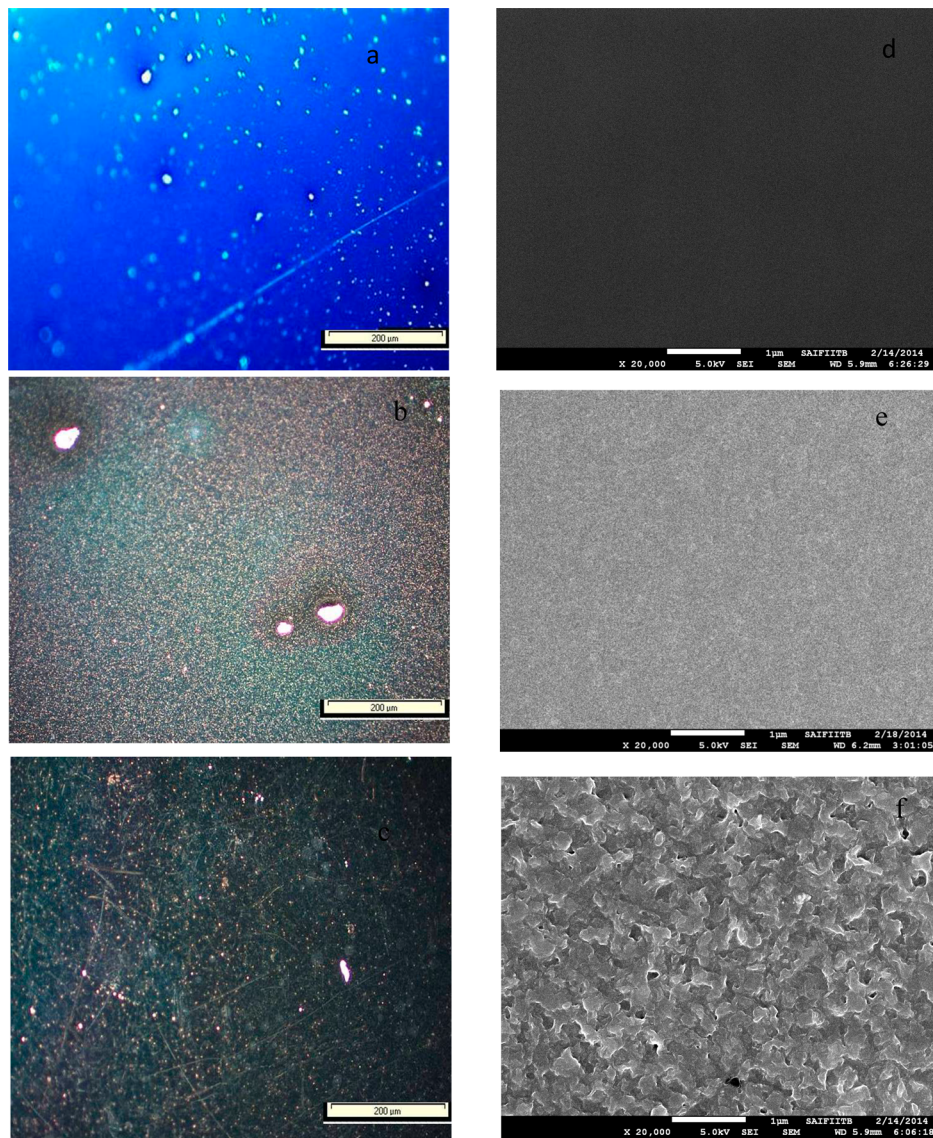


Figure 7. Optical micrographs (a–c) and scanning electron micrographs (d–f) of PANI films on patterned gold coated glass. The images are recorded at (a, d) 0, (b, e) 0.2:1, (c, f) 0.5:1, at ratio of 6CN2/aniline.

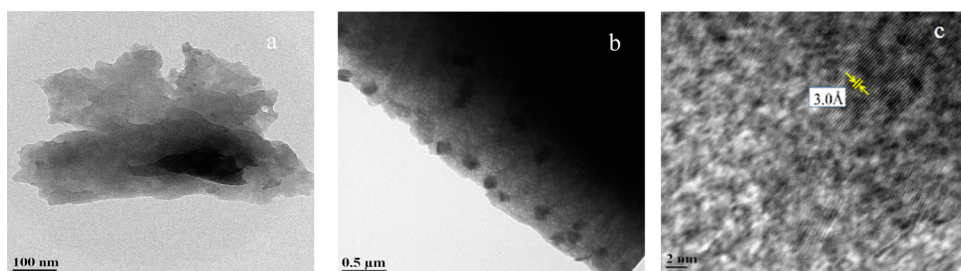


Figure 8. FEGTEM image of (a) PANI-EB films, (b) doped with 6CN2 in the ratio 6CN2/aniline of 0.5:1.0. (c) FEGTEM images of lattice planes of the sample as recorded.

charge carrier tail ($R^2 = 0.999$) is observed in Figure 4b from 600 to 1100 nm region. Figure 4c shows the characteristic charge transfer band between benzenoid to quinoid moieties at 640 nm ($R^2 = 0.985$). The absorption of 6CN2 in NMP, basic, and neutral media were measured and compared with the difference spectrum (obtained from PANI-ES-6CN2 from that of PANI-EB denoted as PANI-ES-6CN2–PANI-EB) (Figure S2c). The neutral and anion absorption peaks of 6CN2 in

NMP were found to be around 300 and 340 nm, respectively. The band at 300 nm was for the neutral species, as confirmed from the absorption measurement in water. The difference spectrum has a maximum at 320 nm, which is red-shifted and broader compared to the band at 300 nm for the neutral form. The amount of neutral species of 6CN2 decreases on protonation of PANI-EB. Also it is observed in Figure S2a that there is an increase in intensity of this 320 nm band in

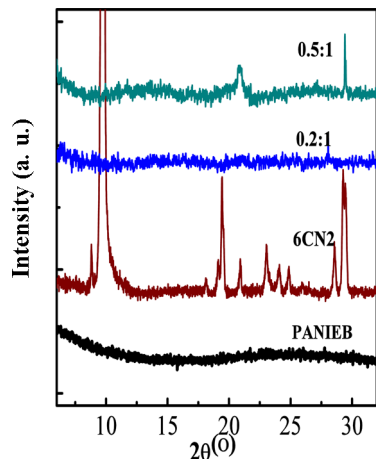


Figure 9. XRD patterns are recorded for PANI-EB, 6CN2, and 6CN2/aniline (0.2:1, 0.5:1).

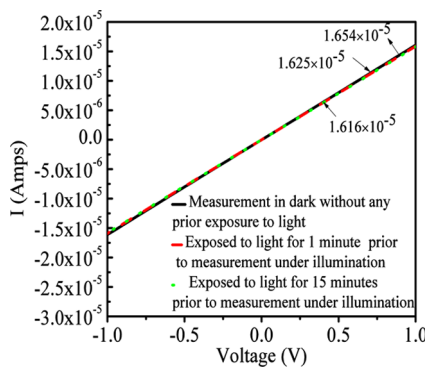


Figure 10. I – V measurements carried out with and without illumination under mercury lamp.

PANI-ES-6CN2 compared to PANI-EB. The reason for this can be accounted from the fact that as PANI-EB gets gradually doped with 6CN2, the absorption at 320 nm is arising from both $\pi-\pi^*$ transition and mostly anion species from 6CN2 (small contribution from neutral species). This was clearly understood when this band was resolved into its components as discussed above. Figure S2d shows 6CN2 has an emission maximum at 400 nm in the solid state. PANI-EB does not show any emission when excited at 310 nm, but the doped form of PANI-ES-6CN2 shows an emission at 400 nm as evident from Figure S2e. The presence of band at 400 nm in the emission spectrum of PANI-ES-6CN2 and the peak at absorption value 450 nm implies the formation of fluorescent PANI-ES.

When the emission spectra of 6CN2 and PANI-ES-6CN2 were resolved and compared with the naphthalate anion spectrum, an interesting peak coincidence of one of the component spectra of PANI-ES-6CN2 with the naphthalate anion is observed at 430 nm. In Figure 6a ($R^2 = 0.993$) both the bands at 384 and 416 nm can be considered to arise from neutral form. Figure 6b ($R^2 = 0.994$) shows the band at 430 nm in the presence of PANI. Again this marks the formation of PANI-ES-6CN2.

Figure 7 shows the morphology of the films. The optical micrograph and the FEGSEM images of undoped PANI-EB are remarkably clear except for the pinholes, thereby confirming the homogeneity of the film (Figure 7a and Figure 7d). The optical micrographs in Figure 7b and Figure 7e show that grainy films are formed with increase in dopant concentration.

When the morphology of the doped films was investigated under FEGSEM, flakelike structures were observed (Figure 7f), indicating the emergence of a microcrystalline phase in the doped film.

Cross-sectional FEGSEM revealed the thickness of the film to be $\sim 32 \mu\text{m}$ (see Supporting Information Figure S1).

This is further manifested in the other characterization techniques. In FEGTEM when the incident beam crosses the sample, part of the beam emerging out of the sample remains unaffected and a part suffers scattering by different processes. It is this scattered beam of electrons that gives information about the chemical, structural, and other properties of the sample.^{37,38} PANI-ES-6CN2 shows nonuniformity in contrast since higher amount of electron scattering is taking place from some regions of the sample. The microcrystallites are clearly visible in FEGTEM images as dark spots that are visible in doped, but not in undoped, PANI-EB (Figure 8a). Dark spots in the lower side of the image (Figure 8b) originate from higher amount of electron diffraction from these areas that can be related to the crystallinity as supported by the lattice planes observed in Figure 8c. Such spots are signatures of microcrystalline domains embedded in an amorphous matrix.³⁹ Also higher amount of contrast difference with the background suggests that these crystalline domains are conducting in nature. Thus, it can be concluded from the FEGTEM images that PANI-ES-6CN2 contains conducting islands in the insulating matrix.⁴⁰ Thus, the conduction can be described as the tunneling between crystalline islands through amorphous bed of the polymer matrix. Higher contrast in the upper side of the image (Figure 8b) is due to difference in thickness of the sample, since higher amount of scattering takes place because of the availability of a large number of electrons. This contrast due to thickness has no relation with the crystallinity or conductance as observed for the dark spots.

Thus, from FEGTEM analysis the conversion of PANI-EB to (PANI-ES-6CN2) is clearly visible. In fact, at the higher magnifications, the lattice planes are clearly visible, with d spacings of $3.0 \pm 0.5 \text{ \AA}$.

Powder XRD of the doped polymer provides further evidence in support of a proton transfer from 6CN2 to PANI. Prior to doping, an almost featureless, broad profile is observed, corresponding to amorphous PANI-EB. Upon doping with 6CN2, distinct peaks appear at 20.77° and 29.41° . The d spacing of $3.0 \pm 0.5 \text{ \AA}$ between the lattice planes, which corresponds to 29.41° , is also visible from FEGTEM. The 20.77° peak is a signature of crystalline PANI-ES, which is the conducting form of the polymer (Figure 9). The emergence of this peak lends credence to the proposed mechanism of protonation of PANI by 6CN2, which is likely to be the cause of the observed enhancement in conductance. A control experiment has been performed on a film of 6CN2, in order to eliminate the possibility that the observed peak is due to the dopant itself. The 6CN2 film exhibited a strong and sharp peak at 9.74° , with sharp peaks for higher values of 2θ , none of which was observed with PANI-ES-6CN2. Thus, it is established that the XRD pattern of the doped film arises from the formation of crystalline domains of PANI-ES. A peak at 29.26° is observed with pure 6CN2, which is close to that at 29.41° , observed for the doped film. The peak at 29.41° may therefore be assigned to the d -spacing corresponding to 6CN2 in PANI-ES-6CN2. From these observations the effect of doping with 6CN2 in PANI structure is clearly manifested. The peak at $2\theta \approx 20.77^\circ$ has a d spacing of 4.2 \AA which represents the interchain

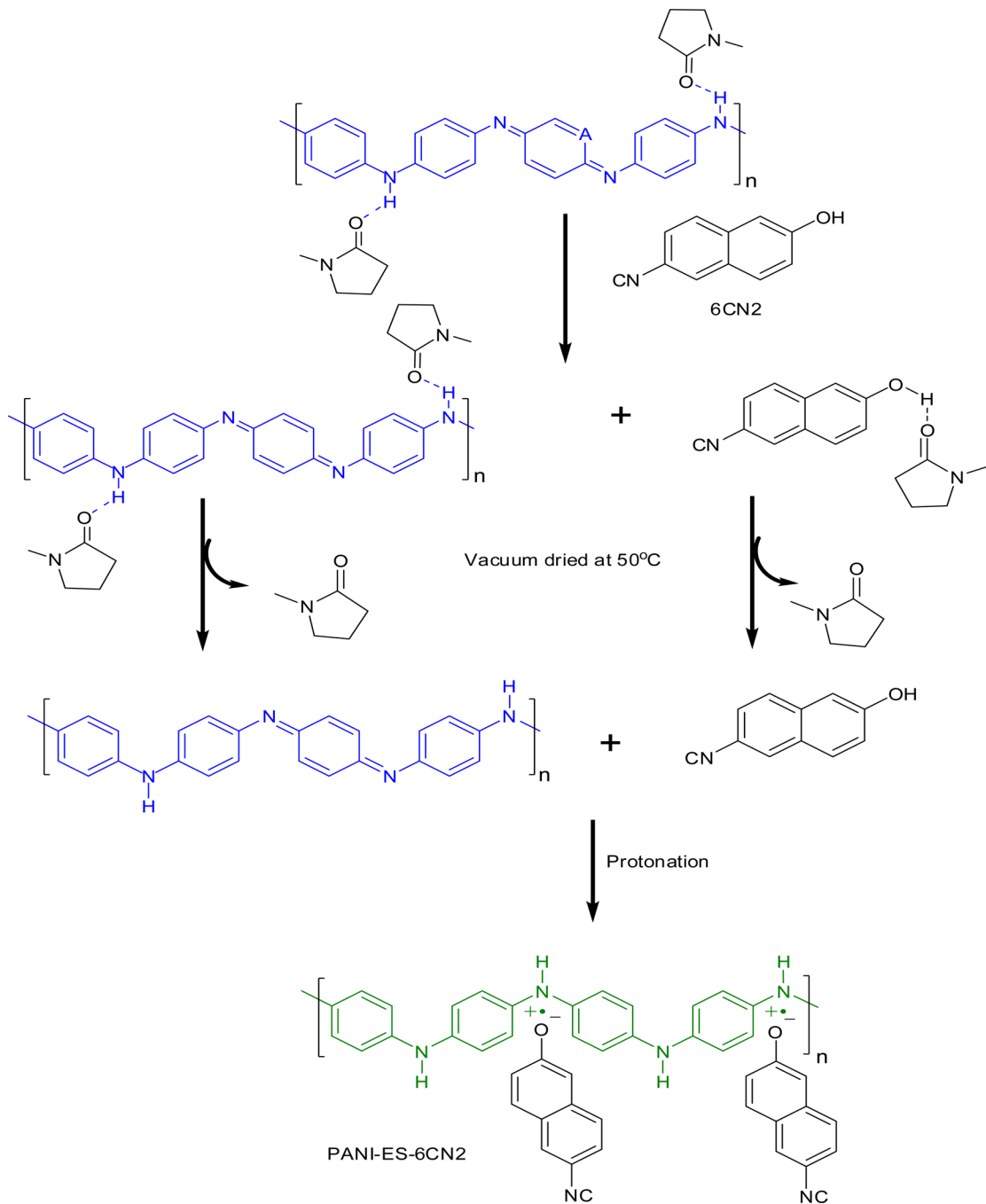


Figure 11. Proposed mechanism supporting formation of PANI-ES-6CN2.

stacking between phenyl rings, thus enhancing the planarity within the polymer.⁴¹

Proposed Mechanism of Doping. We tried to investigate whether the protonation is arising from photodoping or chemical doping. Sample preparations were carried out in the dark for conductance measurements with light. Figure 10 shows results of conductance measurements in the dark and with illumination of the sample by a mercury lamp. Hardly any change in conductance is observed on illumination of the sample. Thus, it seems that protonation is taking place in the ground state itself. The conductance in the dark prior to illumination is already higher ($1.654 \times 10^{-5} \text{ S}$) compared to that of PANI-EB ($6.157 \times 10^{-11} \text{ S}$) for 0.5:1 ratio of 6CN2/aniline. So in the present case, 6CN2 acts as a chemical dopant

rather than a photodopant. Previous literature reports show that in *m*-cresol ($\text{pK}_a = 10$) PANI-EB gets protonated slowly over a period of 1 month.^{42,43} In the present case the protonation was observed in a matter of few hours, upon drying the sample overnight. This makes 6CN2 a better chemical dopant than the phenolic dopants used earlier, even though the pK_a of 6CN2 is 8.4. This is the most surprising result that we have obtained. Interestingly, the protonation does not occur in NMP solutions. It occurs only in solid films. This may be explained as follows: Dissolution of PANI-EB takes place in NMP because of hydrogen bonding as shown in Figure 11.⁴⁴ NMP being a polar aprotic solvent is a hydrogen bond acceptor but not donor. The carbonyl groups of NMP are the only candidates in the molecule that can form hydrogen bonds.

Similarly, the only hydrogen bond donating group in PANI is the N–H moiety. It has been reported earlier that hydrogen bonding exists between these two groups.⁴⁴ This leads to the formation of “blocked structures” as observed in the case of many organic molecules in protic solvents^{45,46} hindering the approach of 6CN2 to the aniline moieties. Besides, 6CN2 would be hydrogen-bonded to NMP molecules as well. Also hydrogen bond formations between 1-naphthol with NMP have been described by Graton et al.⁴⁷ Upon removal of the solvent, the 6CN2 molecules can form a hydrogen bond with the nitrogen atoms of PANI, which is a prerequisite for the protonation–deprotonation process. A similar model has earlier been proposed by Ikkala et al.⁴⁸ and Trznadel et al.⁴³ for dopants like *m*-cresol and camphorsulfonic acid. These models involve stacking of the phenyl rings in addition to hydrogen bonding.

It may be noted that pK_a values of 6CN2 and 2-naphthol are 8.4 and 9.45, respectively, as mentioned before. pK_a value of PANI-ES, on the other hand, has been reported to be 5.0 by Asturias et al.⁴⁹ In their experiments, PANI films were kept in equilibrium with aqueous solutions of different pH. A mere comparison of pK_a values, therefore, would seem to indicate that there should be no proton transfer from 6CN2 to PANI in the ground state of the organic molecule. However, as has been shown by the color, absorption spectrum, and XRD, the PANI-ES-6CN2 is indeed formed and it leaves its signature in the increase in conductance by 6 orders of magnitude. This observation highlights the fact that pK_a , which is strictly defined in aqueous solutions, is not relevant in the solid films of PANI in which our experiments have been performed. In the absence of water and in the presence of a large concentration of basic nitrogen atoms of PANI in the films, proton abstraction by the polymer from the dopant 6CN2 does take place in its ground state.

CONCLUSIONS

The most significant finding of the present study is that rather weak acids like 6CN2 or even 2-naphthol are capable of protonating the nitrogen atoms of PANI-EB, leading to the formation of the PANI-ES and causing a significant enhancement of conductance by 6 orders of magnitude. This observation implies that it is not necessary to use the strong acids that have been used until now, in order to bring about an enhancement in the conductance of PANI. The reason why the protonation of PANI takes place, in spite of its lower pK_a value compared with that of 6CN2, is that there is no water in the system. It is essentially a solid state acid base reaction. Besides, it also tells us that in order to achieve photoconductivity in PANI by this method, one needs to choose an acid that is much weaker, in the ground state, than 6CN2 and even 2-naphthol. To the best of our belief and understanding, this information would be useful in future attempts to achieve the goal of inducing photoconductivity by doping conducting polymers while suppressing dark conductivity. Here we can conclude that 6CN2 protonates PANI-EB to PANI-ES, which brings a change in the morphology, fluorescence, crystallinity, and conducting properties of the polymer. PANI-ES-6CN2 is a luminescent polymer with some amount of crystallinity in it. The crystalline domains that were absent in the amorphous PANI-EB were probably the conducting domains responsible for increase in conductance. The conductance of the PANI-ES-6CN2 was highest for the molar ratio of 0.5:1. Thus, a conducting

fluorescent PANI is synthesized that can have several applications in diverse field.

ASSOCIATED CONTENT

S Supporting Information

Additional data on cross-sectional FEGSEM image of PANI-ES-6CN2 and absorption spectroscopy. This material is available free of charge via the Internet at <http://pubs.acs.org>.

AUTHOR INFORMATION

Corresponding Authors

*A.D.: e-mail, anindya@chem.iitb.ac.in

*A.Q.C.: e-mail, aqcontractor@iitb.ac.in; telephone, +912225767170, +912225767149; fax, +912225767152.

Notes

The authors declare no competing financial interest.

ACKNOWLEDGMENTS

We are grateful to the Departments of Metallurgical Engineering & Materials Science and Electrical Engineering and SAIF IIT Bombay for support in characterization of samples. It is a pleasure to acknowledge Professor S. Dhar for helping with the conductance measurements. D.D. thanks IIT Bombay for a Teaching Assistantship.

REFERENCES

- (1) Kanungo, M.; Kumar, A.; Contractor, A. Q. Microtubule Sensors and Sensor Array Based on Polyaniline Synthesized in the Presence of Poly(styrene sulfonate). *Anal. Chem.* **2003**, *75*, 5673–5679.
- (2) Li, Dan.; Huang, J.; Kaner, R. B. Polyaniline Nanofibers: A Unique Polymer Nanostructure for Versatile Applications. *Acc. Chem. Res.* **2009**, *42*, 135–145.
- (3) Chandrasekhar, P. *Conducting Polymers, Fundamentals and applications: A Practical Approach*; Kluwer Academic Publishers: Boston, MA, 1999.
- (4) MacDiarmid, A. G.; Epstein, A. J. Secondary Doping in Polyaniline. *Synth. Met.* **1995**, *69*, 85–92.
- (5) Varela-Álvarez, A.; Sordo, J. A.; Scuseria, G. E. Doping of Polyaniline by Acid–Base Chemistry: Density Functional Calculations with Periodic Boundary Conditions. *J. Am. Chem. Soc.* **2005**, *127*, 11318–11327.
- (6) MacDiarmid, A. G.; Chiang, J.-C.; Huang, W.; Humphrey, B. D.; Somasiri, N. L. D. Polyaniline: Protonic Acid Doping to the Metallic Regime. *Mol. Cryst. Liq. Cryst.* **1985**, *125*, 309–318.
- (7) Jayakannan, M.; Amrutha, S. R.; Sindhu, K. V. Effect of Composition on the Conductivity and Morphology of Ligno Sulfonic Acid Sodium Salt Doped Polyaniline. *J. Appl. Polym. Sci.* **2006**, *101*, 2650–2655.
- (8) Jeong, S. K.; Suh, J. S.; Oh, E. J.; Park, Y. W.; Kim, C. Y.; MacDiarmid, A. G. Preparation of Polyaniline Free Standing Film by Controlled Processing and Its Transport Property. *Synth. Met.* **1995**, *69*, 171–172.
- (9) Kulszewicz-Bajer, I.; Proń, A.; Abramowicz, J.; Jeandey, C.; Oddou, J.-L.; Sobczak, J. W. Lewis Acid Doped Polyaniline: Preparation and Spectroscopic Characterization. *Chem. Mater.* **1999**, *11*, 552–556.
- (10) Sapargin, A. V.; Brenneman, K. R.; Lee, W. P.; Long, S. M.; Kohlman, R. S.; Epstein, A. J. Li⁺ Doping-Induced Localization in Polyaniline. *Synth. Met.* **1999**, *100*, 55–59.
- (11) Chen, S.-A.; Lin, L.-C. Polyaniline Doped by the New Class of Dopant, Ionic Salt: Structure and Properties. *Macromolecules* **1995**, *28*, 1239–1245.
- (12) Dimitriev, O. P.; Kislyuk, V. V. Interaction of the Europium Chloride and Polyaniline: Formation of a Novel Conductive Complex. *Synth. Met.* **2002**, *132*, 87–92.

- (13) Matnishyan, A. A.; Akhnazaryan, T. L.; Abagyan, G. V.; Badalyan, G. R.; Petrosyan, S. I.; Kravtsova, V. D. Synthesis and Study of Polyaniline Nanocomposites with Metal Oxides. *Phys. Solid State* **2011**, *53*, 1727–1731.
- (14) Bairi, V. G.; Warford, B. A.; Bourdo, S. E.; Biris, A. S.; Viswanathan, T. Synthesis and Characterization of Tanninsulfonic Acid Doped Polyaniline–Metal Oxide Nanocomposites. *J. Appl. Polym. Sci.* **2012**, *124*, 3320–3328.
- (15) Singla, M. L.; Awasthi, S.; Srivastava, A.; Jain, D. V. S. Effect of Doping of Organic and Inorganic Acids on Polyaniline/Mn₃O₄ Composite for NTC and Conductivity Behaviour. *Sens. Actuators, A* **2007**, *136*, 604–612.
- (16) Rana, U.; Chakrabarti, K.; Malik, S. In Situ Preparation of Fluorescent Polyaniline Nanotubes Doped with Perylene Tetracarboxylic Acids. *J. Mater. Chem.* **2011**, *21*, 11098–11100.
- (17) Rana, U.; Chakrabarti, K.; Malik, S. Benzene Tetracarboxylic Acid Doped Polyaniline Nanostructures: Morphological, Spectroscopic and Electrical Characterization. *J. Mater. Chem.* **2012**, *22*, 15665–15671.
- (18) Dhawan, S. K.; Trivedi, D. C. Electrochemical Behaviour of Polyaniline in Aromatic Sulphonic Acids. *Polym. Int.* **1991**, *25*, 55–60.
- (19) Neoh, K. G.; Pun, M. Y.; Kang, E. T.; Tan, K. L. Polyaniline Treated with Organic Acids: Doping Characteristics and Stability. *Synth. Met.* **1995**, *73*, 209–215.
- (20) Kulkarni, M. V.; Viswanath, A. K.; Marimuthu, R.; Seth, T. Synthesis and Characterization of Polyaniline Doped with Organic Acids. *J. Polym. Sci., Part A: Polym. Chem.* **2004**, *42*, 2043–2049.
- (21) Liao, Y.; Zhang, C.; Zhang, Y.; Strong, V.; Tang, J.; Li, X.-G.; Kalantar-zadeh, K.; Hoek, E. M. V.; Wang, K. L.; Kaner, R. B. Carbon Nanotube/Polyaniline Composite Nanofibers: Facile Synthesis and Chemosensors. *Nano Lett.* **2011**, *11*, 954–959.
- (22) Du, Y.; Shen, S. Z.; Yang, W.; Donelson, R.; Cai, K.; Casey, P. S. Simultaneous Increase in Conductivity and Seebeck Coefficient in a Polyaniline/Graphene Nanosheets Thermoelectric Nanocomposite. *Synth. Met.* **2012**, *161*, 2688–2692.
- (23) Huppert, D.; Tolbert, L. M.; Linares-Samaniego, S. Ultrafast Excited-State Proton Transfer from Cyano-Substituted 2-Naphthols. *J. Phys. Chem. A* **1997**, *101*, 4602–4605.
- (24) Tolbert, L. M.; Haubrich, J. E. Enhanced Photoacidities of Cyanonaphthols. *J. Am. Chem. Soc.* **1990**, *112*, 8163–8165.
- (25) Tolbert, L. M.; Haubrich, J. E. Photoexcited Proton Transfer from Enhanced Photoacids. *J. Am. Chem. Soc.* **1994**, *116*, 10593–10600.
- (26) Bhandari, H.; Singh, S.; Choudhary, V.; Dhawan, S. K. Conducting Films of Poly(aniline-co-1-amino-2-naphthol-4-sulfonic acid) Blended with LDPE for Its Application as Antistatic Encapsulation Material. *Polym. Adv. Technol.* **2011**, *22*, 1319–1328.
- (27) Bhandari, H.; Bansal, V.; Choudhary, V.; Dhawan, S. K. Influence of Reaction Conditions on the Formation of Nanotubes/Nanoparticles of Polyaniline in the Presence of 1-Amino-2-naphthol-4-sulfonic Acid and Applications as Electrostatic Charge Dissipation Material. *Polym. Int.* **2009**, *58*, 489–502.
- (28) Rehan, H. H. A New Polymer/Polymer Rechargeable Battery: Polyaniline/LiClO₄ (MeCN)/Poly-1-naphthol. *J. Power Sources* **2003**, *113*, 57–61.
- (29) Venugopal, G.; Quan, X.; Johnson, G. E.; Houlihan, F. M.; Chin, E.; Nalamasu, O. Photoinduced Doping and Photolithography of Methyl-Substituted Polyaniline. *Chem. Mater.* **1995**, *7*, 271–276.
- (30) Kang, Y.; Kim, S. K.; Lee, C. Doping of Polyaniline by Thermal Acid–Base Exchange Reaction. *Mater. Sci. Eng., C* **2004**, *24*, 39–41.
- (31) Duke, C. B.; Conwell, E. M.; Paton, A. Localized Molecular Excitons in Polyaniline. *Chem. Phys. Lett.* **1986**, *131*, 82–86.
- (32) Zhang, Y.; Liu, J.; Yu, W. L.; Huang, D. H.; Li, H. Free-End Boundary Condition and Exciton of an Emeraldine-Base Polymer. *Phys. Status Solidi* **2002**, *231*, 256–262.
- (33) Dimitriev, O. P.; Kislyuk, V. V.; Smertenko, P. S. Intrachain Confinement of Excitons and Radiative Recombination in Polyaniline Grains. *Org. Electron.* **2007**, *8*, 286–291.
- (34) Kumar, D. Spectroscopic Investigations of Substituted Polyaniline. *Indian J. Chem. Technol.* **2002**, *9*, 118–122.
- (35) Xia, Y.; Wiesinger, J. M.; MacDiarmid, A. G. Camphorsulfonic Acid Fully Doped Polyaniline Emeraldine Salt: Conformations in Different Solvents Studied by an Ultraviolet/Visible/Near-Infrared Spectroscopic Method. *Chem. Mater.* **1995**, *7*, 443–445.
- (36) Gospodinova, N.; Muşat, V.; Kolev, H.; Romanova, J. New Insight into the Redox Behavior of Polyaniline. *Synth. Met.* **2011**, *161*, 2510–2513.
- (37) Williams, D. B.; Carter, C. B. *Transmission Electron Microscopy: A Textbook for Materials Science*; Springer Science: New York, NY, U.S., 2009.
- (38) Tong, W. M.; Brodie, A. D.; Mane, A. U.; Sun, F.; Kidwingira, F.; McCord, M. A.; Bevis, C. F.; Elam, J. W. Nanoclusters of MoO_{3x} Embedded in an Al₂O₃ Matrix Engineered for Customizable Mesoscale Resistivity and High Dielectric Strength. *Appl. Phys. Lett.* **2013**, *102*, 252901-1–252901-5.
- (39) Leite, F. L.; Alves, W. F.; Mir, M.; Mascarenhas, Y. P.; Herrmann, P. S. P.; Mattoso, L. H. C.; Oliveira, O. N., Jr. TEM, XRD and AFM Study of Poly(*o*-ethoxyaniline) Films: New Evidence for the Formation of Conducting Islands. *Appl. Phys. A: Mater. Sci. Process.* **2008**, *93*, 537–542.
- (40) Lux, F.; Hinrichsen, G.; Krinichnyi, V. I.; Nazarova, I. B.; Cheremisow, S. D.; Pohl, M.-M. Conducting Islands Concept for Highly Conductive Polyaniline—Recent Results of TEM-, X-ray-Diffraction-, EPR-, D.C. Conductivity- and Magnetic Susceptibility-Measurements. *Synth. Met.* **1993**, *55*, 347–352.
- (41) Varma, S. J.; Xavier, F.; Varghese, S.; Jayalekshmi, S. Synthesis and Studies of Exceptionally Crystalline Polyaniline Thin Films. *Polym. Int.* **2012**, *61*, 743–748.
- (42) Kulikov, A. V.; Komissarova, A. S.; Shestakov, A. F.; Fokeeva, L. S. Spin Crossover in Polyaniline. *Russ. Chem. Bull., Int. Ed.* **2007**, *56*, 2026–2033.
- (43) Trznadel, M.; Rannou, P. Effect of Solvent-Dopant Competition on the Conductivity of Polyaniline Films. *Synth. Met.* **1999**, *101*, 842.
- (44) Ponzi, E. A.; Echevarria, R.; Morales, G. M.; Barbero, C. Removal of *N*-Methylpyrrolidone Hydrogen Bonded to Polyaniline Free-Standing Films by Protonation–Deprotonation Cycles or Thermal Heating. *Polym. Int.* **2001**, *50*, 1180–1185.
- (45) Sarkar, N.; Das, K.; Das, S.; Datta, A.; Nath, D.; Bhattacharyya, K. Excited-State Intramolecular Proton Transfer of 2-(2'-Hydroxyphenyl)benzimidazole in Micelles. *J. Phys. Chem.* **1995**, *99*, 17711–17714.
- (46) Sengupta, P. K.; Kasha, M. Excited State Proton-Transfer Spectroscopy of 3-Hydroxyflavone and Quercetin. *Chem. Phys. Lett.* **1979**, *68*, 382–385.
- (47) Graton, J.; Besseau, F.; Brossard, A.-M.; Charpentier, E.; Deroche, A.; Questel, J.-Y. L. Hydrogen-Bond Acidity of OH Groups in Various Molecular Environments (Phenols, Alcohols, Steroid Derivatives, and Amino Acids Structures): Experimental Measurements and Density Functional Theory Calculations. *J. Phys. Chem. A* **2013**, *117*, 13184–13193.
- (48) Ikkala, O. T.; Pietilä, L.-O.; Ahjopalo, L.; Österholm, H.; Passiniemi, P. J. On the Molecular Recognition and Associations between Electrically Conducting Polyaniline and Solvents. *J. Chem. Phys.* **1995**, *103*, 9855–9863.
- (49) Asturias, G. E.; Jang, G.-W.; MacDiarmid, A. G.; Doblhofer, K.; Zhong, C. Membrane-Properties of Polymer Films: The Acid-Doping Reaction of Polyaniline. *Ber. Bunsen-Ges. Phys. Chem.* **1991**, *95*, 1381–1384.